Published March 4, 2002

JCB Article

The role of cell cycle–regulated expression in the localization of spatial landmark proteins in yeast

Laura R. Schenkman,[1,2] Carlo Caruso,[1,2] Nicolas Pagé,[3] and John R. Pringle[1,2]

[1]Department of Biology and [2]Program in Molecular Biology and Biotechnology, University of North Carolina, Chapel Hill, NC 27599
[3]Department of Biology, McGill University, Montreal H3A 1B1, Canada

In *Saccharomyces cerevisiae,* Bud8p and Bud9p are homologous plasma membrane glycoproteins that appear to mark the distal and proximal cell poles, respectively, as potential sites for budding in the bipolar pattern. Here we provide evidence that Bud8p is delivered to the presumptive bud site (and thence to the distal pole of the bud) just before bud emergence, and that Bud9p is delivered to the bud side of the mother-bud neck (and thence to the proximal pole of the daughter cell) after activation of the mitotic exit network, just before cytokinesis. Like the delivery of Bud8p, that of Bud9p is actin dependent; unlike the delivery of Bud8p, that of Bud9p is also septin dependent. Interestingly, although the transcription of *BUD8* and *BUD9* appears to be cell cycle regulated, the abundance of *BUD8* mRNA peaks in G2/M and that of *BUD9* mRNA peaks in late G1, suggesting that the translation and/or delivery to the cell surface of each protein is delayed and presumably also cell cycle regulated. The importance of time of transcription in localization is supported by promoter-swap experiments: expression of Bud8p from the *BUD9* promoter leads to its localization predominantly to the sites typical for Bud9p, and vice versa. Moreover, expression of Bud8p from the *BUD9* promoter fails to rescue the budding-pattern defect of a *bud8* mutant but fully rescues that of a *bud9* mutant. However, although expression of Bud9p from the *BUD8* promoter fails to rescue a *bud9* mutant, it also rescues only partially the budding-pattern defect of a *bud8* mutant, suggesting that some feature(s) of the Bud8p protein is also important for Bud8p function. Experiments with chimeric proteins suggest that the critical element(s) is somewhere in the extracytoplasmic domain of Bud8p.

Introduction

A central feature of cellular morphogenesis is cell polarization, which involves the asymmetric organization of the cytoskeleton, secretory system, and plasma membrane components along an appropriate axis (Drubin and Nelson, 1996). In the budding yeast *Saccharomyces cerevisiae*, such polarization allows asymmetric growth to form a bud, which becomes the daughter cell. An important feature of cell polarization is the selection of an axis. In *S. cerevisiae*, this is manifested in the selection of bud sites, which occurs in two distinct patterns depending on cell type (Hicks et al., 1977; Chant and Pringle, 1995). In the axial pattern, as seen in normal haploid cells, the daughter cell's first bud forms adjacent to the division site (as marked by the birth scar), and each subsequent bud forms adjacent to the immediately preceding bud site (as marked by the bud scar). This pattern appears to depend on a transient cortical marker that involves the Bud3p, Bud4p, and Axl2p/Bud10p proteins (Chant and Herskowitz, 1991; Chant and Pringle, 1995; Chant et al., 1995; Halme et al., 1996; Roemer et al., 1996a; Sanders and Herskowitz, 1996; Sanders et al., 1999; Lord et al., 2000); during each cell cycle, this marker is deposited at the mother-bud neck and then distributed to the division site on both mother and daughter cells.

In contrast, the bipolar pattern, as seen in normal diploid cells, appears to depend on persistent markers that are deposited at both the birth-scar-distal and birth-scar-proximal poles of the daughter cell, as well as at the division site on the mother cell (Chant and Pringle, 1995). These markers can direct bud formation to the marked site either in the next cell cycle or in a later one. A screen for mutants defective specifically in bipolar bud-site selection led to the identification of the *BUD8* and *BUD9* genes, whose mutant phenotypes suggest that they encode components of the markers at the distal and proximal

The online version of this article contains supplemental material.

Address correspondence to John R. Pringle, Dept. of Biology, CB #3280, 421 Fordham Hall, University of North Carolina, Chapel Hill, NC 27599. Tel.: (919) 962-2293. Fax: (919) 962-0320. E-mail: jpringle@email.unc.edu

N. Pagé's present address is Swiss Institute for Experimental Cancer Research, 1066 Epalinges/VD, Switzerland.

Key words: cell polarity; cell cycle; budding; septins; transmembrane proteins

The Journal of Cell Biology, Volume 156, Number 5, March 4, 2002 829–841
http://www.jcb.org/cgi/doi/10.1083/jcb.200107041

Supplemental Material can be found at:
/content/suppl/2002/02/28/jcb.200107041.DC1.html

Published March 4, 2002

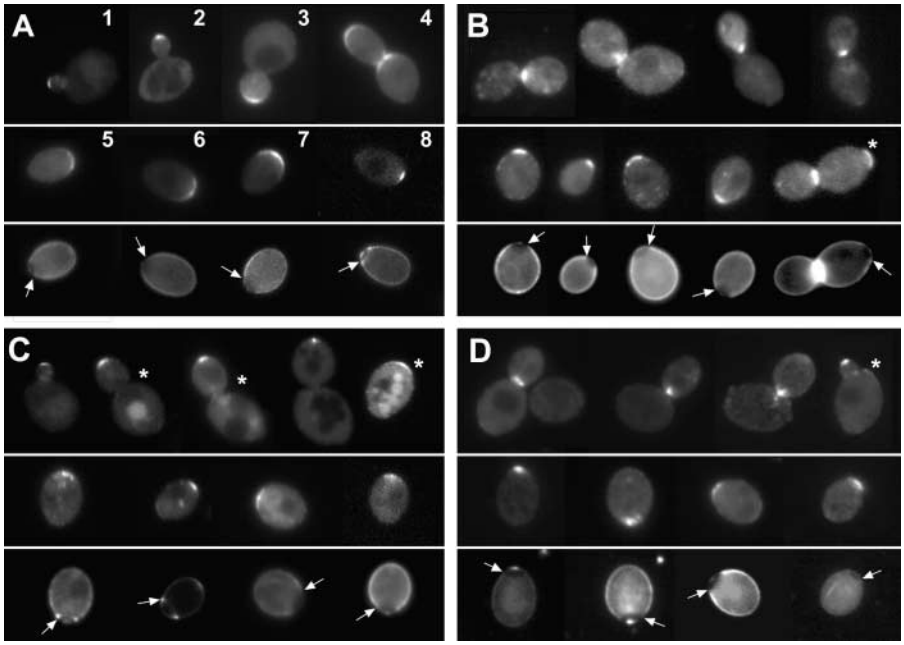

Figure 1. **Localization of GFP–Bud8p and GFP–Bud9p when expressed from their normal promoters (A and B) or the heterologous promoters (C and D).** *bud8-Δ1/bud8-Δ1* strain YHH415 (A and C) and *bud9-Δ1/bud9-Δ1* strain YHH615 (B and D) were transformed with plasmid YEpGFP*–BUD8F (A), YEpGFP*–BUD9 (B), YEpP_{BUD8}GFP*–BUD9 (C), or YEpP_{BUD9}GFP*–BUD8 (D), grown to exponential phase, stained with Calcofluor as described in Materials and methods, and viewed by fluorescence microscopy for GFP and Calcofluor. In each panel, GFP images are displayed in the top and middle sections, and the bottom section shows the Calcofluor staining of the cells shown in the middle section. The birth scars marking the proximal poles are indicated by arrows. Numbers and asterisks indicate cells discussed in the text.

poles of the daughter cell, respectively (Zahner et al., 1996; Harkins et al., 2001). The biochemical properties and localizations of Bud8p and Bud9p are consistent with this hypothesis. Both proteins appear to be integral membrane proteins of the plasma membrane, and each protein consists of a long, heavily glycosylated, NH_2-terminal extracytoplasmic domain followed, at the COOH terminus, by two apparent transmembrane domains bracketing a cytoplasmic domain of ~40 amino acids. The Bud8p and Bud9p cytoplasmic domains are very similar to each other in sequence and presumably provide the recognition sites for the Rsr1p/Bud2p/Bud5p GTPase signaling module, which appears to transmit the positional information from the axial and bipolar cortical markers to the proteins responsible for cell polarization (Pringle et al., 1995; Roemer et al., 1996b; Chant, 1999; Park et al., 1999; Kang et al., 2001; Marston et al., 2001). As expected (Chant and Pringle, 1995; Amberg et al., 1997), Bud8p appears to be localized primarily to the presumptive bud site, the distal pole of the bud, and the distal pole of the daughter cell (Taheri et al., 2000; Harkins et al., 2001). In addition, although Bud9p has also been reported to localize to the distal pole (Taheri et al., 2000), other data suggest strongly that it actually localizes primarily to the bud side of the mother-bud neck and thence to the proximal pole of the daughter cell (Harkins et al., 2001; this study).

In this study, we investigated when and how the very similar Bud8p and Bud9p proteins are localized to the opposite poles of the cell. We found that Bud8p is delivered to the bud site early in the cell cycle, whereas Bud9p is delivered to the neck just before cell division. The timing and site of localization of each protein appear to depend primarily on when in the cell cycle its gene is transcribed.

Results

Sites and timing of normal Bud8p and Bud9p localization

In previous studies, although Bud8p and Bud9p each localized primarily to the expected pole (Introduction), each protein was also observed in some cells at the site expected for the other (Taheri et al., 2000; Harkins et al., 2001). It seemed likely that these unexpected features of Bud8p and Bud9p localization were artifacts of overexpression of the proteins and/or of expression at inappropriate times in the cell cycle. Thus, we reexamined the localization of these proteins using reagents and procedures that were improved in several respects. First, plasmids were constructed using a triple-mutant green fluorescent protein (GFP)* variant that resulted in brighter and more stable signals. Second, because our previously used *GFP–BUD8* construct contained only 290 bp of *BUD8* upstream sequences, which might have truncated the promoter and thus caused mistimed and/or abnormal levels of expression, we constructed plasmids that contained additional *BUD8* upstream sequence (a total of 1410 bp; see Supplemental materials and methods, available at http://www.jcb.org/cgi/content/full/jcb.200107041/DC1). (Although we showed that constructs with 290 bp of upstream sequence could rescue the *bud8* mutant phenotype [Harkins et al., 2001], Mösch and Fink [1997] had identified a *bud8* mutant with a transposon insertion 565 bp upstream of the start codon, suggesting that the *BUD8* promoter might be ≥565 bp in length.) Third, observations were made using a sensitive CCD camera and appropriate image-processing software. Even with these procedures, we were unable to observe strong or consistent signals when the GFP fusion proteins were expressed from low-copy plasmids. However, using high-copy plasmids, we obtained results that were more consistent from cell to cell, simpler, and more easily reconciled with other evidence about the functions of Bud8p and Bud9p.

As in our previous studies, we observed GFP–Bud8p primarily at the tips of buds of various sizes and at the distal poles and nascent budding sites on unbudded cells (Fig. 1

*Abbreviations used in this paper: GFP, green fluorescent protein; Lat A, Latrunculin A.

Published March 4, 2002

A, cells 1–8). A detectable GFP-Bud8p signal was observed at the bud tip in 54% ($n = 254$) of budded cells, whereas a detectable signal was present at one pole in 44% ($n = 234$) of unbudded cells (61% of unbudded daughters; $n = 200$). Virtually no unbudded cells were observed with GFP–Bud8p signal at both poles, and the pole with signal was always the distal pole (Fig. 1 A, cells 5–8). Moreover, the unbudded cells with a GFP–Bud8p signal were essentially all newborn daughter cells (with no bud scars), a result that was expected given that daughter cells nearly always make their first buds at their distal poles (Chant and Pringle, 1995) and that the Bud8p at that pole appears to pass to the bud during bud emergence (Harkins et al., 2001). In addition, as observed previously, GFP–Bud8p was sometimes detected at the mother-bud neck (Fig. 1 A, cell 4). However, in contrast to our previous observations, such signal was now observed infrequently (13% of the 254 budded cells counted) and was always on the mother side, rather than the bud side, of the neck, consistent with the absence of unbudded daughter cells with GFP–Bud8p signal at their proximal poles. A signal was observed at the neck only in large-budded cells (~25% of such cells), and was seen only in cells that also had a detectable patch of GFP–Bud8p at the bud tip.

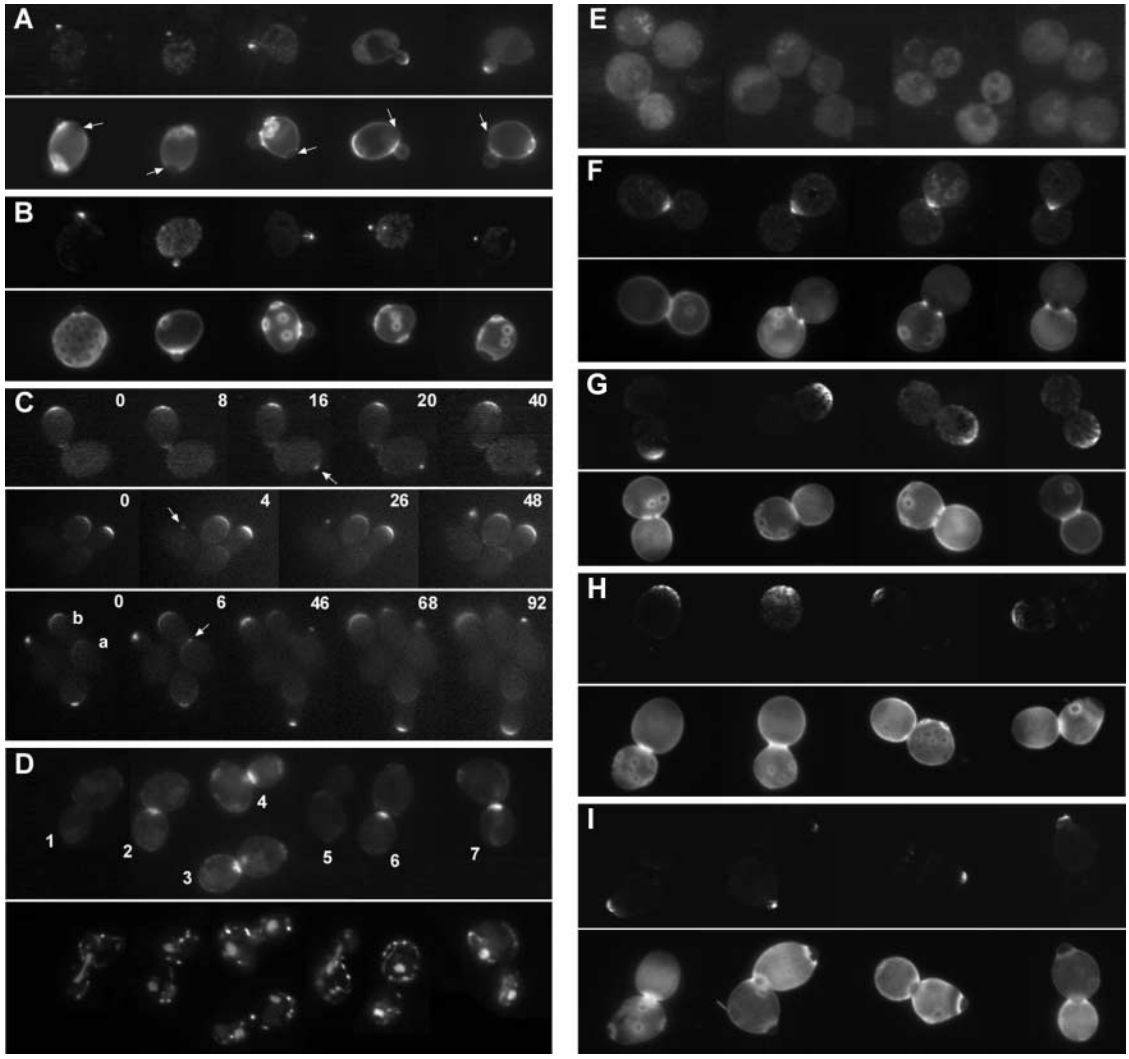

Figure 2. **Localization of GFP–Bud8p to bud sites early in the cell cycle and of GFP–Bud9p to the neck late in the cell cycle.** *bud8-Δ1/bud8-Δ1* strain YHH415 (A and C), *rsr1-Δ2/rsr1-Δ2* strain LSY388 (B), and *cdc15-2* strain cdc15 (G–I) were transformed with plasmid YEpGFP*–BUD8F; *bud9-Δ1/bud9-Δ1* strain HH615 (D) and strain cdc15 (E and F) were transformed with plasmid YEpGFP*–BUD9. (A, B, and D) Cells were grown to exponential phase and stained with Calcofluor (A and B) or DAPI (D) as described in Materials and methods. Individual cells were then imaged for GFP (top section of each panel) and either Calcofluor or DAPI (bottom section of each panel). Arrows indicate birth scars, and numbers indicate cells discussed in the text. (C) Time-lapse observations (Materials and methods) on three groups of cells; times of images (in minutes) are indicated. Note that the quality of focus at particular sites varies from frame to frame. In particular, the presumptive bud site and emerging bud on cell *a* are well focused at 6, 46, and 92 min, but not at 68 min, whereas the distal pole of cell *b* is well focused at 6 min and fairly well focused at 46 and 68 min, but out of focus at 92 min. Arrows indicate the nascent bud sites referred to in the text. (E–I) Cells were arrested at 37°C and released as described in Materials and methods. (E and G, top section) GFP images of arrested cells. (G, bottom section) Calcofluor images of cells in the top section. (F, H, and I) GFP (top sections) and Calcofluor (bottom sections) images of individual cells observed at 45 (F and H) or 60 (I) min after release at 23°C.

Published March 4, 2002

As observed previously (Harkins et al., 2001), the diffuse patch of GFP–Bud8p at the distal pole of the newborn daughter cell became a tighter, brighter patch just before bud emergence at that site (Fig. 1, compare cell 8 to cells 5–7; and Fig. 2 C, cell b). It was difficult to tell whether the tighter patch represented coalesced older material, newly delivered material, or both. Because nearly all daughter cells make their first buds at their distal poles, this also made it difficult to answer the more general question of whether new Bud8p is normally delivered to the bud site at the time of bud emergence. Previously, we had observed that starved cells with no detectable GFP–Bud8p signal developed a tight patch of GFP–Bud8p at the presumptive bud site before bud emergence after refeeding (Harkins et al., 2001). We now extended these observations in several ways. First, after staining normal cells with Calcofluor, we could find cells with tight, bright GFP–Bud8p patches at the tips of small buds in various positions relative to the distal pole and on mother cells of various ages (Fig. 2 A). Similar observations (Fig. 2 B) were made using an *rsr1* mutant strain, which buds in random locations (Bender and Pringle, 1989). Finally, in time-lapse experiments, we observed tight patches of GFP–Bud8p appearing approximately coincident with bud emergence at bud sites remote from the distal pole and/or on previously budded mother cells (Fig. 2 C, arrows). Taken together, the results suggest strongly that whatever the fate of the older Bud8p, new Bud8p is delivered to the nascent bud site shortly before or coincident with bud emergence.

As in our previous studies, we observed GFP–Bud9p at the bud side of the neck in budded cells and at the proximal poles of unbudded cells (Fig. 1 B). Only large-budded cells had detectable GFP–Bud9p signal at the neck, and signal was observed in 25% (n = 200) of such cells. (Much higher percentages were observed in experiments using synchronized cells, as described below). 46% (n = 228) of unbudded cells had detectable GFP–Bud9p at the proximal pole, and these cells were nearly all newborn daughter cells (Fig. 1 B). The signal at the proximal pole was still detectable in 29% (n = 204) of daughter cells during the first budding cycle (Fig. 1 B, *), but it was only rarely detected (<1%) in cells budding for the second or third time. In contrast to our previous observations (made using *GFP–BUD9* expressed from the *GAL* promoter), in the present studies we rarely observed GFP–Bud9p at bud tips or the distal poles of unbudded cells.

The absence of detectable GFP–Bud9p at the neck in small-budded cells suggested that Bud9p is delivered to the neck late in the cell cycle. To investigate this issue further, we first examined exponentially growing cells that had been stained with DAPI to reveal their nuclear morphology. In cells that had not completed anaphase, we never observed GFP–Bud9p at the neck (Fig. 2 D, cells 1 and 5). In contrast, 58% (n = 207) of cells that had completed anaphase had detectable GFP–Bud9p at the neck (Fig. 2 D, cells 2–4, 6, and 7). We then examined cells that had been arrested by a temperature-sensitive mutation in *CDC15,* whose product is a component of the mitotic exit network that controls exit from mitosis and entry into cytokinesis (Morgan, 1999; Lee et al., 2001; McCollum and Gould, 2001; Menssen et al., 2001). The arrested cells displayed no GFP–Bud9p at their necks (Fig. 2 E). However, within 45 min of return to permissive temperature, 68% (n = 201) of the cells displayed GFP–Bud9p at the bud side of the neck (Fig. 2 F). In a parallel experiment, *cdc15* cells expressing GFP–Bud8p showed a broad patch of signal at the distal pole of the bud during arrest at restrictive temperature (Fig. 2 G). Upon return to permissive temperature, no concentration of GFP–Bud8p was observed at the neck before division (Fig. 2 H), although, as expected, tight patches of GFP–Bud8p were observed at the nascent bud sites in the following cell cycle (Fig. 2 I). Thus, most or all new Bud9p appears to be delivered to the neck very late in the cell cycle, just before cytokinesis, and the delivery of Bud8p and Bud9p appears to be under different cell cycle control.

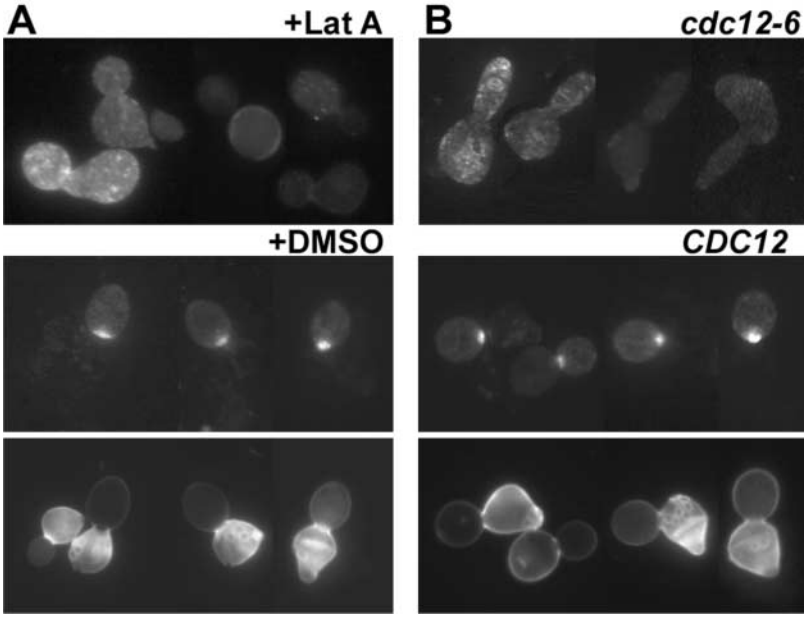

Figure 3. **Dependence of GFP–Bud9p localization on actin and the septins.** (A) Strain ML130 (*MATa bar1*Δ) was transformed with YEpGFP*–BUD9, synchronized with α factor, grown for 70 min, and treated for 20 min with Lat A in DMSO or with DMSO alone as described in Materials and methods. (Top and middle panels) GFP images; (bottom panel) Calcofluor images of the cells shown in the middle panel. (B) Strains ML130 and LSY192 (*MATa bar1*Δ *cdc12-6*) were transformed with YEpGFP*–BUD9, synchronized with α factor, and then incubated for 90 min at 37°C as described in Materials and methods. (Top and middle panels) GFP images; (bottom panel) Calcofluor images of the cells shown in the middle panel.

Published March 4, 2002

Actin and septin dependence of Bud9p localization

As integral-membrane proteins, Bud8p and Bud9p are presumably delivered to the plasma membrane in vesicles derived from the secretory system. Both early in the cell cycle (when Bud8p appears to be delivered) and late in the cell cycle (when Bud9p appears to be delivered), polarized delivery of secretory vesicles to the cell surface appears to depend largely on the actin cytoskeleton (Lew and Reed, 1995; Drubin and Nelson, 1996; Pruyne and Bretscher, 2000a, 2000b). Consistent with this model, we observed previously that GFP–Bud8p delivery to presumptive bud sites was abolished in cells whose F-actin was ablated by treatment with Latrunculin A (Lat A) (Harkins et al., 2001). Similarly, treatment with Lat A also abolished the delivery of GFP–Bud9p to the neck late in the cell cycle (Fig. 3 A; in the DMSO-only control, 59% [$n = 200$] of the cells showed GFP–Bud9p at the neck), indicating that this delivery is also actin dependent. In addition, experiments with a temperature-sensitive septin mutant indicated that delivery of Bud9p to the neck is also septin dependent (Fig. 3 B). In contrast, delivery of Bud8p to presumptive bud sites and bud tips appeared to be unaffected by disruption of the septin/scaffold (Harkins et al., 2001).

Role of cell cycle–regulated expression in Bud8p and Bud9p localization and function

Although Bud8p and Bud9p are structurally similar proteins, it is possible that targeting signals within the polypeptides may cause (or contribute to) their distinct localizations. However, the data described above suggested that timing of expression might also be important for localization and function. Consistent with this possibility, microarray analyses have indicated that the *BUD8* and *BUD9* mRNAs accumulate at distinct times in the cell cycle (Cho et al., 1998; Spellman et al., 1998). To explore this possibility further, we first reanalyzed the *BUD8* and *BUD9* mRNA levels through the cell cycle using Northern blotting and two different methods of synchronization. In general agreement with the microarray analyses, we observed that *BUD8* mRNA peaks in G2/M, coincident with *CLB2* mRNA, whereas *BUD9* mRNA peaks in late G1, coincident with *CLN2* mRNA (Fig. 4 A). Although consistent with the hypothesis that differential timing of gene expression is important for the distinct functions of Bud8p and Bud9p, these results were also surprising in that each mRNA peaked long before the corresponding protein appears to be delivered to the cell surface.

To test directly whether the timing of gene expression is critical for the localization and/or function of Bud8p and Bud9p, we then constructed plasmids and strains in which an untagged or tagged copy of each gene was expressed from the promoter of the other gene. To confirm that exchanging the promoters really did alter the timing of gene expression, we examined RNA from a synchronized population of cells that had both a normal *BUD8* locus and a P_{BUD9}*HA-BUD8* construct in place of the *BUD9* locus. As expected, the *HA-BUD8* mRNA showed a peak in late G1 (Fig. 4 B), the time at which *BUD9* mRNA normally peaks (see above).

We next examined the function of the chimeric genes by evaluating their abilities to rescue the *bud8* and *bud9* mutant phenotypes. As expected, the absence of proximal-pole budding in a *bud9/bud9* strain (Fig. 5, A, panel 1, and B, panel 1) could be rescued by a plasmid containing a normal *BUD9* gene (Fig. 5 B, panel 2; this budding pattern was essentially the same as that in wild-type cells [Harkins et al., 2001]). In contrast, neither low-copy (unpublished data) nor high-copy (Fig. 5 B, panel 3) *BUD8* expressed from its own promoter could rescue the *bud9/bud9* mutant phenotype. Remarkably, however, low-copy plasmids expressing either untagged or tagged *BUD8* from the *BUD9* promoter could rescue proximal-pole budding in the mutant strain (Fig. 5, A, panel 2, and B, panels 4 and 6). In contrast, a plasmid expressing *BUD9* itself from the *BUD8* promoter could not rescue the mutant

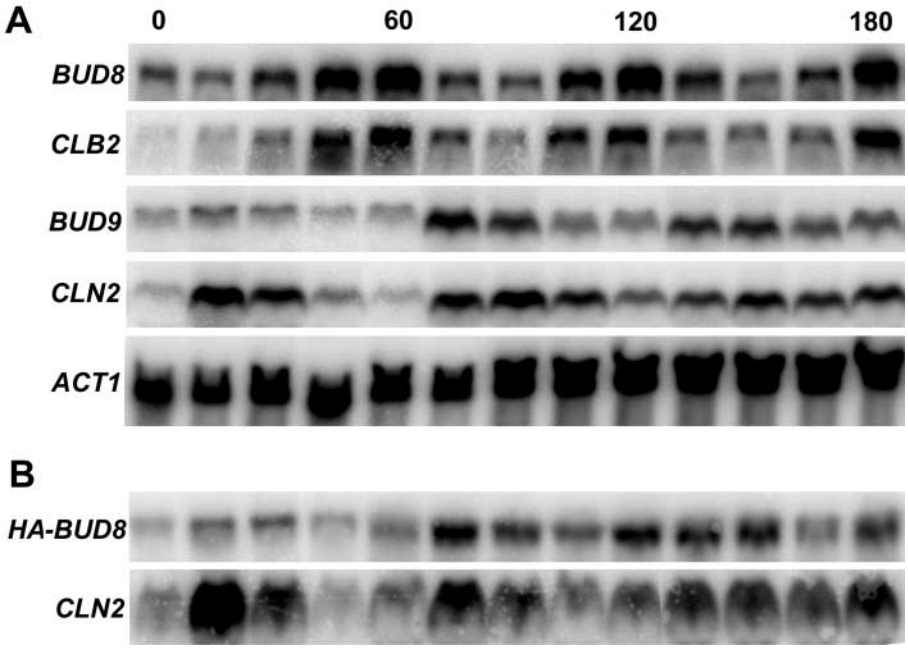

Figure 4. ***BUD8* and *BUD9* expression through the cell cycle.** *BUD8 BUD9* strain LSY90 (A) and *BUD8 bud9-Δ::HA-BUD8* strain LSY305 (B) were synchronized with α factor as described in Materials and methods. Total RNAs were extracted from samples taken at 15-min intervals and analyzed by Northern blotting using probes specific for the indicated genes (Materials and methods). Similar results were obtained when RNAs from strain cdc15 were analyzed after synchronization by *cdc15* arrest and release (Materials and methods). In B, the use of a probe specific for the HA-epitope sequences allows specific detection of message from the *bud9-Δ::HA-BUD8* locus despite the presence of normal *BUD8* mRNA.

Published March 4, 2002

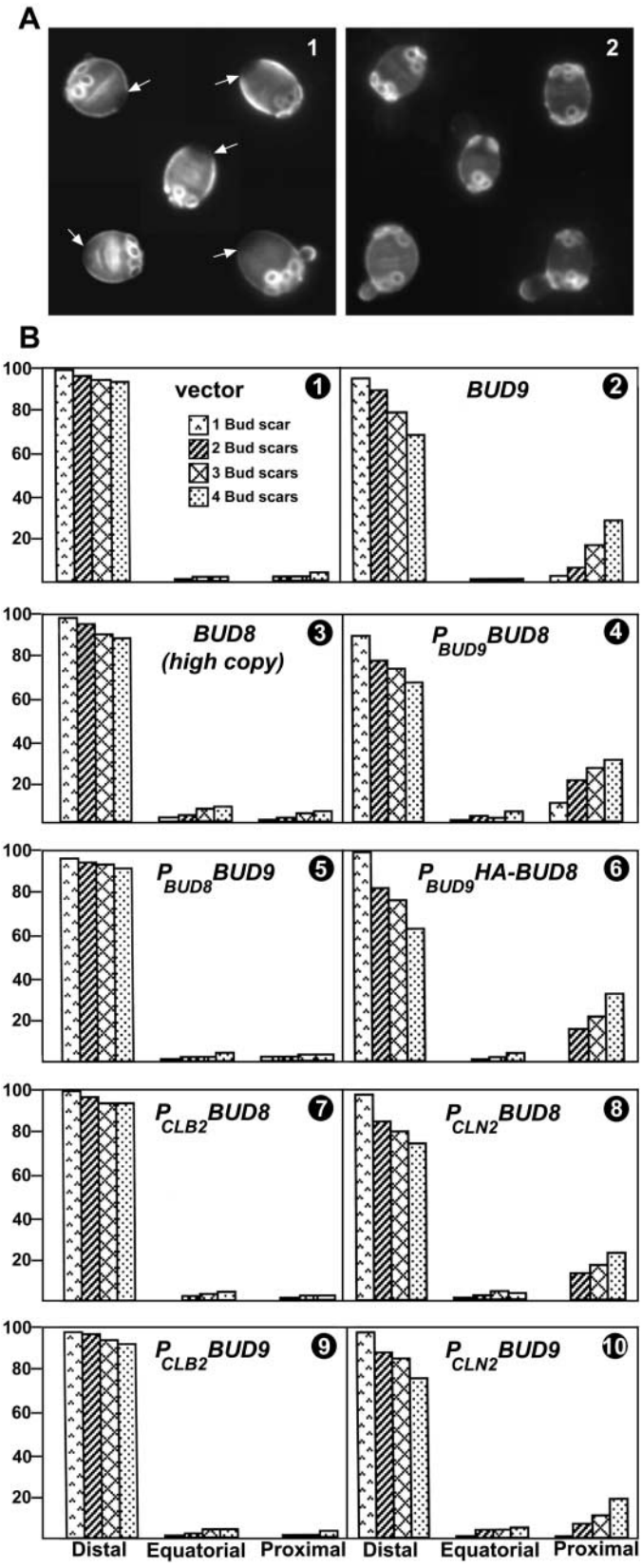

Figure 5. **Rescue of a *bud9* mutant by either *BUD9* or *BUD8* if expressed early in the cell cycle.** Exponentially growing cells were stained with Calcofluor to evaluate budding patterns. (A) Fluorescence micrographs of *bud9-Δ1/bud9-Δ1* strain YHH615 harboring (1) control plasmid YCplac111 or (2) P_{BUD9}*BUD8* plasmid YCpP_{BUD9}BUD8. Arrows indicate the birth scars marking the proximal poles. (B) Quantitative evaluation of budding patterns. For each strain, the positions of all bud scars were determined for 100 cells with one bud scar (i.e., 100 total bud scars), 100 cells with two bud scars (i.e., 200 total bud scars), 100 cells with three bud scars (i.e., 300 total bud scars), and 100 cells with four bud scars (i.e., 400 total bud scars). Bud scars were scored as distal (the third of the cell most distal to the birth scar), equatorial (the middle third of the cell), or proximal (the third of the cell surrounding the birth scar). For each strain, the average value from three independent experiments is shown. (1-5 and 7–10) Strain YHH615 harboring plasmid (1) YCplac111, (2) YCpBUD9, (3) YEpBUD8, (4) YCpP_{BUD9}BUD8, (5) YCpP_{BUD8}BUD9, (7) YCpP_{CLB2}BUD8, (8) YCpP_{CLN2}BUD8, (9) YCpP_{CLB2}BUD9, or (10) YCpP_{CLN2}BUD9. (6) *bud9-Δ1/bud9-Δ::HA-BUD8* strain LSY492.

phenotype (Fig. 5 B, panel 5). As expected if expression in late G1 is critical for *BUD9* function, either *BUD8* or *BUD9* could partially rescue the phenotype of the *bud9/bud9* strain when expressed from the *CLN2* promoter but not when expressed from the *CLB2* promoter (Fig. 5 B, panels 7–10).

Consistent with these tests of function, when GFP–Bud8p was expressed from the *BUD9* promoter, signal was observed predominantly in the locations normal for Bud9p (Fig. 1 D), despite the potential complications arising from the need to use a high-copy plasmid in these experiments. In particular,

Published March 4, 2002

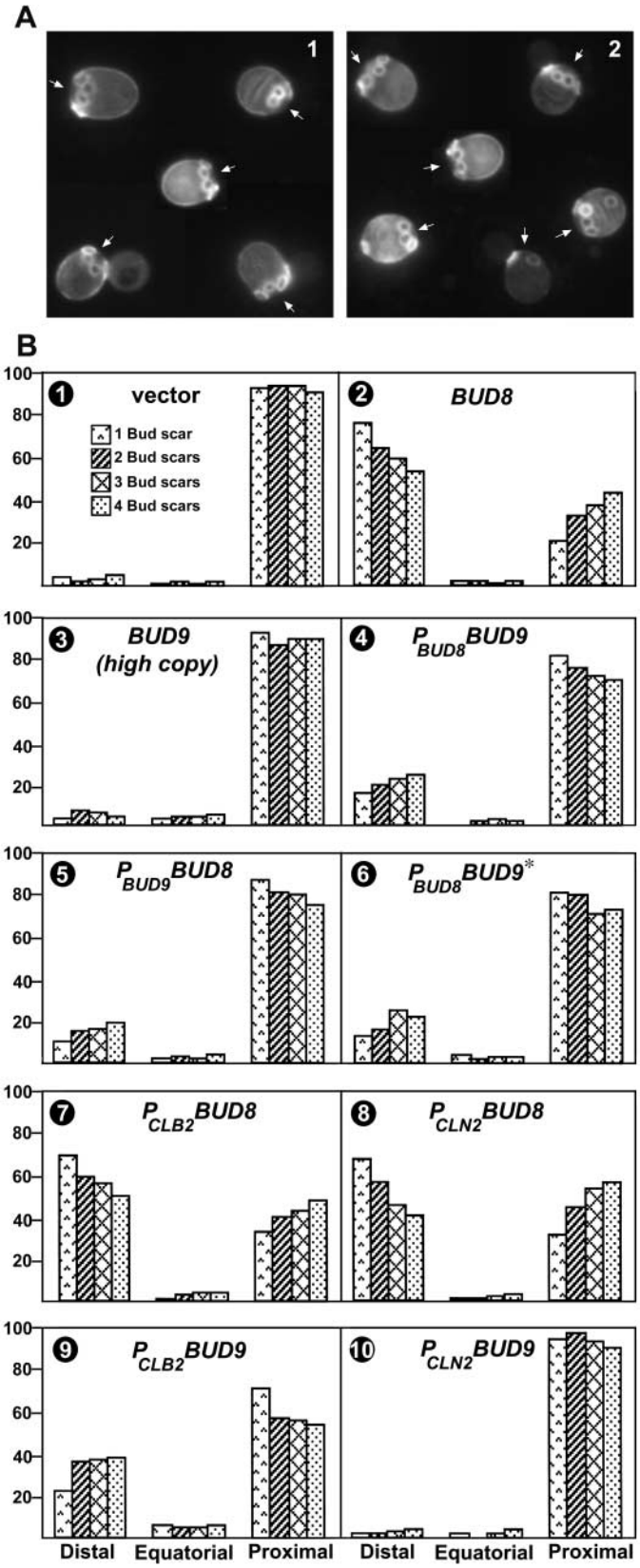

Figure 6. **Rescue of a *bud8* mutant by *BUD8* if expressed late in the cell cycle and partial rescue by *BUD8* if expressed early in the cell cycle or *BUD9* if expressed late.** Exponentially growing cells were stained with Calcofluor, and budding patterns were evaluated as in Fig. 5. (A) Fluorescence micrographs of *bud8-Δ1/bud8-Δ1* strain YHH415 harboring (1) control plasmid YCplac111 or (2) P_{BUD8}*BUD9* plasmid YCpP_{BUD8}BUD9. Arrows indicate the birth scars marking the proximal poles. (B) Quantitative evaluation of budding patterns in strain YHH415 harboring plasmid (1) YCplac111, (2) YCpBUD8, (3) YEpBUD9, (4) YCpP_{BUD8}BUD9, (5) YCpP_{BUD9}BUD8, (6) YCpP_{BUD8}BUD9*, (7) YCpP_{CLB2}BUD8, (8) YCpP_{CLN2}BUD8, (9) YCpP_{CLB2}BUD9, or (10) YCpP_{CLN2}BUD9. Plasmids YCpP_{BUD8}BUD9 and YCpP_{BUD8}BUD9* contain downstream sequences from *BUD9* and *BUD8*, respectively.

27% (n = 218) of large-budded cells (but no small-budded cells) had detectable GFP–Bud8p signal at the daughter side of the neck, whereas 67% (n = 239) of unbudded daughter cells had signal at the proximal pole. In addition, 15% (n = 410) of small-budded cells and 24% (n = 404) of large-budded cells had detectable GFP–Bud8p signal at the bud tip (Fig. 1 D, *). However, these signals were typically rather faint, and daughter cells with detectable signal at the distal pole were rare: just 2.5% (n = 440) of unbudded cells had signal detectable at both poles or at the distal pole only.

Published March 4, 2002

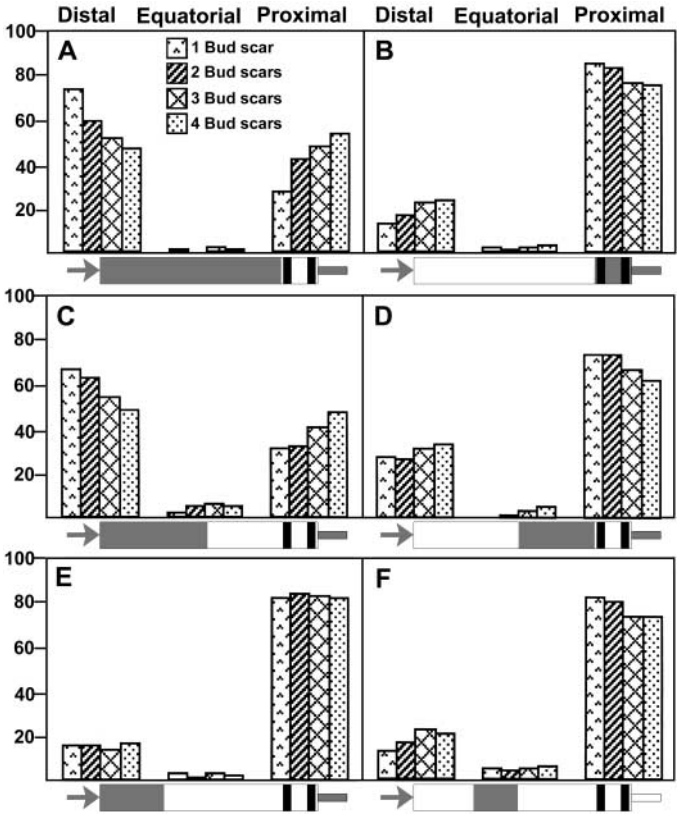

Figure 7. **Dependence of Bud8p function on sequences in its extracytoplasmic domain.** Exponentially growing cells of *bud8-Δ1/bud8-Δ1* strain YHH415 harboring various plasmids were stained with Calcofluor, and budding patterns were evaluated quantitatively as described in Fig. 5. The plasmids contain *BUD8/BUD9* chimeras as diagrammed in the figure and described in the Supplemental materials and methods (available at http://www.jcb.org/cgi/content/full/jcb.200107041/DC1). *BUD8* regions of the chimeric open reading frames are gray; *BUD9* regions are white. Black bars indicate the transmembrane domains. Each chimera contains the *BUD8* promoter (gray arrow) and *BUD8* (A–E, solid gray line) or *BUD9* (F, white line) downstream sequences. Plasmids used were (A) YCpBUD8/9-1, (B) YCpBUD8/9-2, (C) YCpBUD8/9-3, (D) YCpBUD8/9-4, (E) YCpBUD8/9-5, and (F) YCpBUD8/9-6.

Given the results just described, it was surprising that the reciprocal experiments presented a more complicated picture. As expected, the absence of distal-pole budding in a *bud8/bud8* strain (Fig. 6, A, panel 1, and B, panel 1) could be rescued by a plasmid containing a normal *BUD8* gene (Fig. 6 B, panel 2; this budding pattern was nearly the same as that in wild-type cells [Harkins et al., 2001]). In contrast, neither low-copy (unpublished data) nor high-copy (Fig. 6 B, panel 3) *BUD9* expressed from its own promoter could rescue the *bud8/bud8* mutant phenotype. However, although a plasmid expressing *BUD8* from the *BUD9* promoter also rescued distal-pole budding only poorly (Fig. 6 B, panel 5), plasmids expressing *BUD9* from the *BUD8* promoter (with either the *BUD8* or *BUD9* downstream sequences) were only slightly more effective (Fig. 6, A, panel 2, and B, panels 4 and 6). Moreover, although as expected, a plasmid expressing *BUD8* from the *CLB2* promoter rescued distal-pole budding well (Fig. 6 B, panel 7), and a plasmid expressing *BUD9* from the *CLN2* promoter showed no rescue (Fig. 6 B, panel 10), a plasmid expressing *BUD9* from the *CLB2* promoter showed only partial rescue of distal-pole budding (Fig. 6 B, panel 9) and was actually somewhat less effective than a plasmid expressing *BUD8* from the *CLN2* promoter (Fig. 6 B, panel 8). Although these results are difficult to interpret in detail, they do suggest that effective Bud8p function requires some aspects of the Bud8p protein that are not fully shared by Bud9p.

Despite these complications, examination of cells expressing GFP–Bud9p from the *BUD8* promoter confirmed the importance of the promoter in determining the localization of the protein. In particular, under these conditions, GFP–Bud9p was seen only at the tips of buds and at the distal poles of daughter cells (Fig. 1 C), and never in the normal Bud9p locations, consistent with the failure of P_{BUD8}*BUD9* to rescue proximal-pole budding in a *bud9/bud9* strain (see above). Moreover, the GFP–Bud9p signals seen upon expression from the *BUD8* promoter were considerably weaker (and detectable in a smaller fraction of the cells) than for the other cases considered here, suggesting that the failure of P_{BUD8}*BUD9* to effectively rescue distal-pole budding in a *bud8/bud8* mutant strain might reflect inefficient delivery of Bud9p to the normal Bud8p location, poor stability once there, or both. Some support for this hypothesis was provided by the observation that in some cells expressing GFP–Bud9p from the *BUD8* promoter, a signal was detected in internal vesicles (Fig. 1 C, asterisks).

Functional dissection of Bud8p

In an attempt to determine what portion(s) of Bud8p are necessary to have effective Bud8p function, we constructed several genes expressing chimeric Bud8p/Bud9p proteins from the *BUD8* promoter and tested their abilities to rescue distal-pole budding in a *bud8/bud8* mutant strain. Interestingly, a protein comprised of the extracytoplasmic domain of Bud8p and the transmembrane and cytoplasmic domains of Bud9p rescued the *bud8/bud8* mutant phenotype essentially as well as did full-length Bud8p (Fig. 7 A; compare Fig. 6 B, panel 2), whereas the reciprocal construct rescued no better than did the expression of full-length Bud9p from the *BUD8* promoter (Fig. 7 B; compare Fig. 6 B, panel 4). Thus, the transmembrane and cytoplasmic domains of Bud8p and Bud9p appear to be interchangeable, and the

Published March 4, 2002

special feature(s) of Bud8p appear to lie in the extracytoplasmic domain. Analysis of additional chimeras suggested that both the NH_2-terminal and COOH-terminal halves of the Bud8p extracytoplasmic domain contribute to Bud8p function (Fig. 7, C and D; compare and A and B, respectively) and that a region near the middle of the domain is important (Fig. 7 E) but not sufficient (Fig. 7 F) for effective Bud8p function.

Discussion

Several lines of evidence suggest strongly that Bud8p and Bud9p play central roles in marking the distal and proximal poles of the daughter cell, respectively, as potential sites for budding in the bipolar pattern (Introduction). However, it should be noted that each spatial landmark may also involve other proteins; for example, it appears that Rax2p may also form part of the mark at the proximal pole (Chen et al., 2000). In this study, we investigated when and how the structurally similar Bud8p and Bud9p are delivered to the opposite poles of the cell. Although there remain caveats resulting from our inability to visualize the proteins consistently at normal levels of expression, our results indicate that Bud8p is normally delivered to the nascent bud site shortly before or coincident with bud emergence, whereas Bud9p is normally delivered to the bud side of the neck very late in the cell cycle, after activation of the mitotic exit network and just before cytokinesis. These are the times at which secretory vesicles are delivered to these sites by the actin cytoskeleton (Lew and Reed, 1995; Drubin and Nelson, 1996; Pruyne and Bretscher, 2000a,b), so it is not surprising that the localization of both Bud8p (Harkins et al., 2001) and Bud9p (this study) to the appropriate sites is actin dependent. In addition, because localization of proteins to the neck typically depends on the septins (Gladfelter et al., 2001), it is not surprising that the localization of Bud9p is also septin dependent. The mechanisms by which Bud9p and certain other neck-localized proteins (Gladfelter et al., 2001) become distributed asymmetrically on the septin scaffold remain to be elucidated.

The timing of gene expression appears to be a primary determinant of Bud8p and Bud9p localization and function: when Bud8p is expressed from the *BUD9* promoter, it localizes as if it were Bud9p and appears fully competent to provide Bud9p (but not Bud8p) function. Moreover, when Bud9p is expressed from the *BUD8* promoter, it localizes as if it were Bud8p and is unable to provide Bud9p function. However, under these conditions, the Bud9p localization signal appears weak, and the protein at the distal pole is only partially effective in providing Bud8p function. Thus, there appear to be features of the Bud8p polypeptide itself that are important for its efficient delivery, stability, and/or function at the distal pole. Although these features have not yet been defined in detail, experiments with chimeric proteins indicate that they lie primarily in the central and NH_2-terminal portions of the extracytoplasmic domain. Because it seems likely that the extracellular domains of Bud8p and Bud9p must interact with components of the cell wall in order to maintain the localization of the proteins, it is possible that the special feature(s) of Bud8p allow it to interact effectively with some (unknown) component of the wall at the distal pole.

Consistent with the evidence for a role of cell cycle–regulated expression, the *BUD8* and *BUD9* mRNAs show distinct peaks in abundance during the cell cycle (Cho et al., 1998; Spellman et al., 1998; this study). For several reasons, these peaks are likely to reflect cell cycle–regulated transcription. First, this is the most common mechanism for cell cycle regulation of transcript levels (Spellman et al., 1998). Second, consistent with the apparent times of transcription of the two genes, the *BUD9* upstream sequences contain potential binding sites for the MBF and SBF transcription factors, whereas the *BUD8* upstream sequences contain potential binding sites for the MCM1 + SFF transcription factor (Spellman et al., 1998). Finally, despite the complications that might result from using promoters of different inherent strengths, expression of either Bud8p or Bud9p from the *CLN2* promoter, which is known to drive G1 transcription (Breeden, 1996; Spellman et al., 1998), can provide partial Bud9p function, whereas expression of either protein from the *CLB2* promoter, which is known to drive G2/M transcription (Spellman et al., 1998), can provide partial Bud8p function.

However, these results also raise an important question: Why are the *BUD8* and *BUD9* mRNAs expressed so far in advance of when the corresponding proteins appear to arrive at the cell surface? The experiments involving block and release by a temperature-sensitive mutation affecting the mitotic exit network are particularly intriguing: in the *cdc15*-arrested cells, GFP–Bud9p is not detectable at the cell surface, and GFP–Bud8p is present only as a diffuse patch at the distal pole of the bud (as would be expected from its appearance in large-budded cells during an unperturbed cell cycle). Upon release by return to permissive temperature, GFP–Bud9p appears at the bud side of the neck before cell division, whereas no detectable new delivery of GFP–Bud8p to the cell surface occurs until the beginning of the next cell cycle, when it appears at the nascent bud site in the usual way. The several possible explanations for these observations include cell cycle–regulated delays in mRNA translation (conceivably coupled to a localization of the mRNAs themselves) or in the delivery of Bud8p- and Bud9p-containing secretory vesicles to the cell surface. We cannot yet discriminate between these (or perhaps other) explanations. In further studies of this issue, it will be necessary also to explain how starved cells (which are arrested in G0/G1) (Pringle and Hartwell, 1981) can deliver new Bud8p to the nascent bud site upon refeeding (Harkins et al., 2001) without passing through the stage of the cell cycle in which *BUD8* appears to be transcribed.

A concern in these studies was whether a lag in the development of fluorescence by the GFP-tagged proteins might complicate the interpretation of the results. That is, it seemed possible that Bud8p and/or Bud9p might be translated and delivered to the plasma membrane immediately after the corresponding mRNA was expressed, but that the fluorescence of the tagged proteins might become detectable only later. However, such a model is difficult to reconcile with several features of the available data. First, to explain the appearance of new GFP–Bud8p at the nascent bud site

Published March 4, 2002

just at the time of bud emergence, we would need to assume that protein synthesized in G2/M of one cell cycle could be delivered at that time to the precise spot that would be used for budding in the next cell cycle. This seems quite unlikely, particularly in a case like that of the random-budding *rsr1* mutant. Second, the absence in the *cdc15*-arrested cells of any spot of GFP–Bud8p resembling those seen at new bud sites also appears to argue against the model, as does the appearance of GFP–Bud8p at the nascent bud site when starved cells are refed (Harkins et al., 2001). Third, the absence of GFP–Bud9p at the neck of cells arrested at the *cdc15* block for 3–4 h (about twice the length of the normal cell cycle) is also difficult to reconcile with the model. Although this experiment could be misleading if the GFP has greater difficulty in achieving a fluorescent state at 37°C, we also observed that cells arrested in G2/M at 23°C by nocodazole and benomyl had no detectable GFP–Bud9p at the neck even after 3 h of incubation (unpublished data). Thus, it seems safe to conclude that there really is a substantial delay between the expression of the *BUD8* and *BUD9* mRNAs and the arrival of the proteins at the cell surface.

It has long been known that many yeast genes are expressed in a cell cycle–regulated manner (Johnston, 1990; Breeden, 1996), and recent microarray experiments have indicated that the total of such genes is in the range of 416 (Cho et al., 1998) to 800 (Spellman et al., 1998). However, the functional significance of this regulation has been tested in relatively few cases, and in many cases in which tests have been done, eliminating the cell cycle regulation of transcription has had little or no effect on cell viability or function (Johnston, 1990; Breeden, 1996; Igual et al., 1996; Detweiler and Li, 1997). Thus, *BUD8* and *BUD9* provide important examples of cases in which the timing of transcription does appear to be critical for protein localization and function. Another important example, and an interesting comparison to the case of *BUD8* and *BUD9,* is provided by Axl2p/Bud10p, an integral-membrane component of the cortical marker used in axial budding (Halme et al., 1996; Roemer et al., 1996a). Altering the normal late-G1 expression of *AXL2* results in a severe disruption of protein localization and function, apparently because expression of the *AXL2* mRNA is quickly followed by translation and the delivery of vesicles containing the newly made Axl2p to wherever the general secretory vesicle traffic of the cell is directed at that time in the cell cycle (Lord et al., 2000). Nonetheless, the transport of Axl2p to the cell surface appears to involve distinctive features, because it is affected much more than general secretory traffic by mutations affecting the ER-membrane protein Erv14p (Powers and Barlowe, 1998). Another interesting comparison is provided by the proteins involved in mating-type switching: cell cycle regulation of transcription of the *HO* gene is part of the complex mechanism (involving also the asymmetric localization of the mRNA for the transcriptional repressor Ash1p) by which the HO protein is localized specifically to the mother cell (Bobola et al., 1996; Sil and Herskowitz, 1996; Long et al., 2001; Maxon and Herskowitz, 2001; and references cited therein). It will be interesting to see if there are many other examples in which protein localization (and hence function) depends on the timing of gene expression, and, if so, which types of mechanisms are involved.

Materials and methods

Strains, growth conditions, and genetic and recombinant DNA methods

Yeast strains used in this study are listed in Table I; construction of strains LSY305 and LSY388 is described below. Standard methods of yeast genetics were used (Guthrie and Fink, 1991; Gietz et al., 1992). Except where noted, cells were grown at 23°C on YM-P rich liquid medium, YPD rich solid medium, or synthetic complete (SC) medium lacking appropriate nutrients as needed to maintain plasmids (Lillie and Pringle, 1980; Guthrie and Fink, 1991). All media contained 2% glucose as carbon source. Cells to be examined for GFP fluorescence were grown in the dark to minimize photobleaching.

To synchronize cells as a population of unbudded, G1-phase cells, α factor (Sigma-Aldrich) was added to a final concentration of 30 ng/ml to an exponentially growing culture (~10^7 cells/ml), and incubation was continued for 90 min. For Northern blot analyses (see below), cells were collected by centrifugation at 650 *g* for 5 min at 23°C, resuspended at a similar density in fresh medium without α factor, and incubated further. At intervals, samples were collected by centrifugation at high speed in a table-top centrifuge for 2 min at 23°C, and the pellets were flash frozen in an ethanol/dry ice bath. To investigate the actin dependence of Bud9p localization, Lat A (Molecular Probes) was added to a final concentration of 100 μM from a 20-mM stock solution in DMSO. Lat A (or the same concentration of DMSO alone as a control) was added to the synchronized culture 70 min after the shift back to medium without α factor, and the cells were examined 20 min later. To investigate the septin dependence of Bud9p localization, the α factor–arrested cells were resuspended in fresh medium without α factor that had been prewarmed to 37°C, incubation was continued at 37°C, and cells were examined after 90 min.

Table I. **Strains used in this study**

Strain	Genotype	Source
YEF473	***a****/α his3-Δ200/his3-Δ200 leu2-Δ1/leu2-Δ1 lys2-801/lys2-801 trp1-Δ63/trp1-Δ63 ura3-52/ura3-52*	Bi and Pringle, 1996
YEF473A	***a*** *his3-Δ200 leu2-Δ1 lys2-801 trp1-Δ63 ura3-52*	Segregant from YEF473
YHH415	as YEF473 except *bud8-Δ1/bud8-Δ1*	Harkins et al., 2001
YHH615	as YEF473 except *bud9-Δ1/bud9-Δ1*	Harkins et al., 2001
ML130	as YEF473A except *bar1Δ*	Harkins et al., 2001
LSY192	as YEF473A except *bar1Δ cdc12-6*	Harkins et al., 2001
cdc15	*α cdc15-2* (W303 background)	Spellman et al., 1998
LSY87	as YEF473A except *bar1Δ bud3Δ::HIS3 bud9-Δ1*	This study[a]
LSY90	as YEF473A except *bar1Δ bud3Δ::HIS3*	This study[a]
LSY305	as YEF473A except *bar1Δ bud3Δ::HIS3 bud9-Δ::HA-BUD8*	See text
LSY388	as YEF473 except *rsr1-Δ2/rsr1-Δ2*	See text
LSY492	as YEF473 except *bar1Δ/+ bud3Δ::HIS3/+ bud9-Δ1/bud9-Δ::HA-BUD8*	This study[b]

[a]Segregant from a cross between YHH772 (Harkins et al., 2001) and ML130.
[b]Obtained by mating YHH614 (Harkins et al., 2001) to LSY305.

Published March 4, 2002

Table II. **Plasmids used in this study**

Plasmid	Description[a]	Source
pRS315	*CEN6 ARS4 LEU2* (low copy)	Sikorski and Hieter, 1989
pRS316	*CEN6 ARS4 URA3* (low copy)	Sikorski and Hieter, 1989
YEplac181	*LEU2* (high copy)	Gietz and Sugino, 1988
YEplac195	*URA3* (high copy)	Gietz and Sugino, 1988
YCplac111	*CEN4 ARS1 LEU2* (low copy)	Gietz and Sugino, 1988
YIplac211	*URA3* (integrative)	Gietz and Sugino, 1988
YCpBUD8F	*BUD8* in pRS316	This study
YEpBUD8	*BUD8* in YEplac181[b]	Harkins et al., 2001
YCpBUD9	*BUD9* in YCplac111	Harkins et al., 2001
YEpBUD9	*BUD9* in YEplac195	Harkins et al., 2001
YEpGFP*–BUD8F	*GFP–BUD8* in YEplac181[c]	This study
YEpGFP*–BUD9	*GFP-BUD9* in YEplac195[c]	This study
YCpP_{BUD9}BUD8	P_{BUD9}*BUD8* in YCplac111	This study
YCpP_{BUD8}BUD9	P_{BUD8}*BUD9* in pRS315	This study
YEpP_{BUD8}GFP*–BUD9	P_{BUD8}*GFP–BUD9* in YEplac181[c]	This study
YEpP_{BUD9}GFP*–BUD8	P_{BUD9}*GFP–BUD8* in YEplac195[c]	This study
YIpP_{BUD9}HA-BUD8	P_{BUD9}*HA-BUD8* in YIplac211	This study
YCpP_{BUD8}BUD9*	P_{BUD8}*BUD9* in pRS315[d]	This study
YCpP_{CLB2}BUD8	P_{CLB2}*BUD8* in pRS315	This study
YCpP_{CLN2}BUD8	P_{CLN2}*BUD8* in pRS315	This study
YCpP_{CLB2}BUD9	P_{CLB2}*BUD9* in YCplac111	This study
YCpP_{CLN2}BUD9	P_{CLN2}*BUD9* in YCplac111	This study
YCpBUD8/9-1	chimeric *BUD8/9-1* in pRS315[d,e]	This study
YCpBUD8/9-2	chimeric *BUD8/9-2* in pRS315[d,e]	This study
YCpBUD8/9-3	chimeric *BUD8/9-3* in pRS315[d,e]	This study
YCpBUD8/9-4	chimeric *BUD8/9-4* in pRS315[d,e]	This study
YCpBUD8/9-5	chimeric *BUD8/9-5* in pRS315[d,e]	This study
YCpBUD8/9-6	chimeric *BUD8/9-6* in pRS315[e,f]	This study

[a]Except where indicated, cloned genes are present in DNA fragments that include both their normal promoters and their normal downstream sequences. Except for YEpBUD8, plasmids containing the *BUD8* promoter contain 1410 bp of *BUD8* upstream sequences (see text and Supplemental materials and methods, available at http://www.jcb.org/cgi/content/full/jcb.200107041/DC1).
[b]Contains 290 bp of *BUD8* upstream sequences.
[c]The *GFP* allele encodes GFP with the F64L, S65T, and V163A substitutions.
[d]Contains the *BUD8* downstream sequences.
[e]Contains P_{BUD8}.
[f]Contains the *BUD9* downstream sequences.

To synchronize cells late in the cell cycle using the *cdc15-2* temperature-sensitive mutation, a culture growing exponentially at 23°C was shifted to 37°C and incubated for 3 to 4 h, at which point ~98% of the cells had large buds. To release cells from the arrest, they were collected by centrifugation at 650 *g* for 5 min and resuspended in fresh medium at 23°C.

Plasmids used in this study are listed in Table II and/or described in the Supplemental materials and methods (available at http://www.jcb.org/cgi/content/full/jcb.200107041/DC1). *Escherichia coli* strains DH12S and DH5α (Life Technologies) were used for plasmid maintenance by standard procedures (Sambrook et al., 1989). Standard methods of DNA manipulation were used (Sambrook et al., 1989; Ausubel et al., 1995). PCR was performed using *Taq* DNA polymerase (Promega). Other enzymes were purchased from New England Biolabs, and oligonucleotide primers (Integrated DNA Technologies) are listed in Table III (Supplemental materials and methods, available at http://www.jcb.org/cgi/content/full/jcb.200107041/DC1). DNA sequencing was performed by the UNC-Chapel Hill Automated DNA Sequencing Facility.

Strain constructions

To construct a strain carrying a complete deletion of the *RSR1* ORF, the PCR method (Baudin et al., 1993) was used to replace one wild-type *RSR1* allele in YEF473. Primers LS174 and LS175 were used with plasmid pFA6a-His3MX6 (Wach et al., 1997; Longtine et al., 1998) as template. The presence of the deletion (named *rsr1-Δ2*) was confirmed by PCR (Longtine et al., 1998), and 2:2 segregation of the marker together with a random budding phenotype was observed. Appropriate segregants were mated to obtain the homozygous mutant strain LSY388.

To construct a strain expressing the *HA-BUD8* coding region from the chromosomal *BUD9* promoter, plasmid YIpP_{BUD9}HA-BUD8 was digested with *Hin*dIII (cutting the plasmid once, in the *BUD9* upstream sequence) and transformed into *bud9-Δ1* strain LSY87. A Ura^+ transformant showing restoration of bipolar budding was designated LSY305. PCR using DNA from LSY305 as template and primers LS157 and LS156 (one upstream of the *Hin*dIII site in the *BUD9* upstream sequences, the other within the *BUD8* ORF) confirmed that LSY305 had the desired structure at the *BUD9* locus.

RNA methods

Yeast total RNA was isolated by the hot-phenol extraction method as described by Leeds et al. (1991). For Northern blotting, samples of total RNA were denatured by formamide–formaldehyde treatment fractionated on 1% agarose/formaldehyde gels (Ausubel et al., 1995), and then transferred to Hybond-N+ membranes (Amersham Pharmacia Biotech). Hybridization of DNA probes to these RNA blots was essentially as described by Sambrook et al. (1989). To generate probes specific for *BUD8*, *BUD9*, *CLN2*, *CLB2*, *HA*, or *ACT1*, primer pairs LS93 and LS94, LS95 and LS96, LS112 and LS113, LS114 and LS115, LS158 and LS159, and LS183 and LS184, respectively, were used to amplify DNA fragments by PCR from templates YCpBUD8, YCpBUD9, pGAL-CLN2 (a gift from S. Reed via D. Lew [Duke University, Durham, NC]), pGAL-CLB2 (a gift from S. Reed via D. Lew), YCpHA-BUD9, and pRS316-GAL1-ACT1 (Liu et al., 1992), respectively. To allow normalization of the amounts of RNA per lane, a preliminary blot was probed for *ACT1*, and the signals were quantitated using a Storm 840 Phosphorimager and Imagequant 5.0 software (Molecular Dynamics).

Staining and microscopy

To visualize bud scars and birth scars for the determination of budding patterns, exponentially growing cells were suspended in water containing 1 μg/ml Calcofluor as described by Zahner et al. (1996) and examined on a Nikon Microphot SA microscope using an Apo 60X/1.40 NA oil-immer-

sion objective. To visualize GFP–Bud8p or GFP–Bud9p in living cells, cells were grown to exponential phase in the dark, collected by centrifugation at 23°C, and suspended in water or in water containing 1 μg/ml Calcofluor. To visualize nuclear DNA, the exponentially growing cells were stained by adding DAPI (Sigma-Aldrich) from a 1-mg/ml stock solution in water to a final concentration of 1 μg/ml and continuing to incubate the culture for 90 min before resuspending the cells in water for examination. To prepare slides for time-lapse microscopy, cells growing exponentially in SC-Leu medium were pipetted onto slabs of 2× SC medium (like SC but with all ingredients at twice normal concentration; 2% glucose as carbon source) containing 25% gelatin, and coverslips were applied and sealed with Valap (Salmon et al., 1998). All images for figures were collected using Metamorph software (Universal Imaging Corporation) with a Nikon Eclipse 600 FN microscope equipped with a Hamamatsu ORCA-2 CCD camera and an Apo 100X/1.40 NA oil-immersion objective. Exposure times were set automatically and averaged ~6 s for GFP images except for those of cells expressing GFP–Bud9p from $YEpP_{BUD8}$GFP*–BUD9, which averaged ~15 s. Exposure times for Calcofluor images averaged ~0.2 sec.

Online supplemental material

The online supplement (available at http://www.jcb.org/cgi/content/full/jcb.200107041/DC1) contains the details of plasmid constructions and a table of oligonucleotide primers used.

We thank Amos McKenzie III, Mark Longtine, Dale Beach, David Brenner, Heidi Harkins, I-Ching Yu, Danny Lew, Bruce Futcher, Howard Bussey, and other members of our laboratories for encouragement, helpful discussions, and/or strains and plasmids.

This work was supported by National Institutes of Health Grant GM31006.

Submitted: 10 July 2001
Revised: 18 January 2002
Accepted: 23 January 2002

References

Amberg, D.C., J.E. Zahner, J.W. Mulholland, J.R. Pringle, and D. Botstein. 1997. Aip3p/Bud6p, a yeast actin-interacting protein that is involved in morphogenesis and the selection of bipolar budding sites. *Mol. Biol. Cell.* 8:729–753.

Ausubel, F.M., R. Brent, R.E. Kingston, D.D. Moore, J.G. Seidman, J.A. Smith, and K. Struhl. 1995. Current Protocols in Molecular Biology. John Wiley & Sons, New York.

Baudin, A., O. Ozier-Kalogeropoulos, A. Denouel, F. Lacroute, and C. Cullin. 1993. A simple and efficient method for direct gene deletion in *Saccharomyces cerevisiae*. *Nucleic Acids Res.* 21:3329–3330.

Bender, A., and J.R. Pringle. 1989. Multicopy suppression of the *cdc24* budding defect in yeast by *CDC42* and three newly identified genes including the *ras*-related gene *RSR1*. *Proc. Natl. Acad. Sci. USA.* 86:9976–9980.

Bi, E., and J.R. Pringle. 1996. *ZDS1* and *ZDS2*, genes whose products may regulate Cdc42p in *Saccharomyces cerevisiae*. *Mol. Cell. Biol.* 16:5264–5275.

Bobola, N., R.-P. Jansen, T.H. Shin, and K. Nasymth. 1996. Asymmetric accumulation of Ash1p in postanaphase nuclei depends on a myosin and restricts yeast mating-type switching to mother cells. *Cell.* 84:699–709.

Breeden, L. 1996. Start-specific transcription in yeast. *Curr. Top. Microbiol. Immunol.* 208:95–127.

Chant, J. 1999. Cell polarity in yeast. *Annu. Rev. Cell Dev. Biol.* 15:365–391.

Chant, J., and I. Herskowitz. 1991. Genetic control of bud site selection in yeast by a set of gene products that constitute a morphogenetic pathway. *Cell.* 65: 1203–1212.

Chant, J., and J.R. Pringle. 1995. Patterns of bud-site selection in the yeast *Saccharomyces cerevisiae*. *J. Cell Biol.* 129:751–765.

Chant, J., M. Mischke, E. Mitchell, I. Herskowitz, and J.R. Pringle. 1995. Role of Bud3p in producing the axial budding pattern of yeast. *J. Cell Biol.* 129: 767–778.

Chen, T., T. Hiroko, A. Chaudhuri, F. Inose, M. Lord, S. Tanaka, J. Chant, and A. Fujita. 2000. Multigenerational cortical inheritance of the Rax2 protein in orienting polarity and division in yeast. *Science.* 290:1975–1978.

Cho, R.J., M.J. Campbell, E.A. Winzeler, L. Steinmetz, A. Conway, L. Wodicka, T.G. Wolfsberg, A.E. Gabrielian, D. Landsman, D.J. Lockhart, and R.W. Davis. 1998. A genome-wide transcriptional analysis of the mitotic cell cycle. *Mol. Cell.* 2:65–73.

Detweiler, C.S., and J.J. Li. 1997. Cdc6p establishes and maintains a state of replication competence during G1 phase. *J. Cell Sci.* 110:753–763.

Drubin, D.G., and W.J. Nelson. 1996. Origins of cell polarity. *Cell.* 84:335–344.

Gietz, R.D., and A. Sugino. 1988. New yeast-*Escherichia coli* shuttle vectors constructed with in vitro mutagenized yeast genes lacking six-base pair restriction sites. *Gene.* 74:527–534.

Gietz, D., A. St. Jean, R.A. Woods, and R.H. Schiestl. 1992. Improved method for high efficiency transformation of intact yeast cells. *Nucleic Acids Res.* 20: 1425–1426.

Gladfelter, A.S., J.R. Pringle, and D.J. Lew. 2001. The septin cortex at the yeast mother-bud neck. *Curr. Opin. Microbiol.* 4:681–689.

Guthrie, C., and G.R. Fink. 1991. Guide to Yeast Genetics and Molecular Biology. Methods Enzymol. Vol. 194. Academic Press, San Diego. 933 pp.

Halme, A., M. Michelitch, E.L. Mitchell, and J. Chant. 1996. Bud10p directs axial cell polarization in budding yeast and resembles a transmembrane receptor. *Curr. Biol.* 6:570–579.

Harkins, H.A., N. Pagé, L.R. Schenkman, C. De Virgilio, S. Shaw, H. Bussey, and J.R. Pringle. 2001. Bud8p and Bud9p, proteins that may mark the sites for bipolar budding in yeast. *Mol. Biol. Cell.* 12:2497–2518.

Hicks, J.B., J.N. Strathern, and I. Herskowitz. 1977. Interconversion of yeast mating types. III. Action of the homothallism (*HO*) gene in cells homozygous for the mating type locus. *Genetics.* 85:395–405.

Igual, J.C., A.L. Johnson, and L.H. Johnston. 1996. Coordinated regulation of gene expression by the cell cycle transcription factor SWI4 and the protein kinase C MAP kinase pathway for yeast cell integrity. *EMBO J.* 15:5001–5013.

Johnston, L.H. 1990. Periodic events in the cell cycle. *Curr. Opin. Cell Biol.* 2:274–279.

Kang, P.J., A. Sanson, B. Lee, and H.-O. Park. 2001. A GDP/GTP exchange factor involved in linking a spatial landmark to cell polarity. *Science.* 292:1376–1378.

Lee, S.E., L.M. Frenz, N.J. Weils, A.L. Johnson, and L.H. Johnston. 2001. Order of function of the budding-yeast mitotic exit-network proteins Tem1, Cdc15, Mob1, Dbf2, and Cdc5. *Curr. Biol.* 11:784–788.

Leeds, P., S.W. Peltz, A. Jacobson, and M.R. Culbertson. 1991. The product of the yeast *UPF1* gene is required for rapid turnover of mRNAs containing a premature translational termination codon. *Genes Dev.* 5:2303–2314.

Lew, D.J., and S.I. Reed. 1995. Cell cycle control of morphogenesis in budding yeast. *Curr. Opin. Genet. Dev.* 5:17–23.

Lillie, S.H., and J.R. Pringle. 1980. Reserve carbohydrate metabolism in *Saccharomyces cerevisiae*: responses to nutrient limitation. *J. Bacteriol.* 143:1384–1394.

Liu, H., J. Krizek, and A. Bretscher. 1992. Construction of a *GAL1*-regulated yeast cDNA expression library and its application to the identification of genes whose overexpression causes lethality in yeast. *Genetics.* 132:665–673.

Long, R.M., W. Gu, X. Meng, G. Gonsalvez, R.H. Singer, and P. Chartrand. 2001. An exclusively nuclear RNA-binding protein affects asymmetric localization of *ASH1* mRNA and Ash1p in yeast. *J. Cell Biol.* 153:307–318.

Longtine, M.S., A. McKenzie III, D.J. DeMarini, N.G. Shah, A. Wach, A. Brachat, P. Philippsen, and J.R. Pringle. 1998. Additional modules for versatile and economical PCR-based gene deletion and modification in *Saccharomyces cerevisiae*. *Yeast.* 14:953–961.

Lord, M., M.C. Yang, M. Mischke, and J. Chant. 2000. Cell cycle programs of gene expression control morphogenetic protein localization. *J. Cell Biol.* 151: 1501–1511.

Ma, H., S. Kunes, P.J. Schatz, and D. Botstein. 1987. Plasmid construction by homologous recombination in yeast. *Gene.* 58:201–216.

Marston, A.L., T. Chen, M.C. Yang, P. Belhumeur, and J. Chant. 2001. A localized GTPase exchange factor, Bud5, determines the orientation of division axes in yeast. *Curr. Biol.* 11:803–807.

Maxon, M.E., and I. Herskowitz. 2001. Ash1p is a site-specific DNA-binding protein that actively represses transcription. *Proc. Natl. Acad. Sci. USA.* 98: 1495–1500.

McCollum, D., and K.L. Gould. 2001. Timing is everything: regulation of mitotic exit and cytokinesis by the MEN and SIN. *Trends Cell Biol.* 11:89–95.

Menssen, R., A. Neutzner, and W. Seufert. 2001. Asymmetric spindle pole localization of yeast Cdc15 kinase links mitotic exit and cytokinesis. *Curr. Biol.* 11:345–350.

Morgan, D.O. 1999. Regulation of the APC and the exit from mitosis. *Nat. Cell Biol.* 1:E47–E53.

Mösch, H.-U., and G.R. Fink. 1997. Dissection of filamentous growth by transposon mutagenesis in *Saccharomyces cerevisiae*. *Genetics.* 145:671–684.

Oldenburg, K.R., K.T. Vo, S. Michaelis, and C. Paddon. 1997. Recombination-mediated PCR-directed plasmid construction *in vivo* in yeast. *Nucleic Acids Res.* 25:451–452.

Park, H.-O., A. Sanson, and I. Herskowitz. 1999. Localization of Bud2p, a GTPase-activating protein necessary for programming cell polarity in yeast to the presumptive bud site. *Genes Dev.* 13:1912–1917.

Powers, J., and C. Barlowe. 1998. Transport of Axl2p depends on Erv14p, an ER-vesicle protein related to the *Drosophila cornichon* gene product. *J. Cell Biol.* 142:1209–1222.

Pringle, J.R., and L.H. Hartwell. 1981. The *Saccharomyces cerevisiae* cell cycle. *In* The Molecular Biology of the Yeast *Saccharomyces*. Life Cycle and Inheritance. Strathern, J.N., E.W. Jones, and J.R. Broach, editors. Cold Spring Harbor Laboratory Press, Cold Spring Harbor, New York. 97–142.

Pringle, J.R., E. Bi, H.A. Harkins, J.E. Zahner, C. De Virgilio, and H. Fares. 1995. Establishment of cell polarity in yeast. *Cold Spring Harbor Symp. Quant. Biol*. 60:729–743.

Pruyne, D., and A. Bretscher. 2000a. Polarization of cell growth in yeast. I. Establishment and maintenance of polarity states. *J. Cell Sci.* 113:365–375.

Pruyne, D., and A. Bretscher. 2000b. Polarization of cell growth in yeast. II. The role of the cortical actin cytoskeleton. *J. Cell Sci.* 113:571–585.

Roemer, T., K. Madden, J. Chang, and M. Snyder. 1996a. Selection of axial growth sites in yeast requires Axl2p, a novel plasma membrane glycoprotein. *Genes Dev.* 10:777–793.

Roemer, T., L.G. Vallier, and M. Snyder. 1996b. Selection of polarized growth sites in yeast. *Trends Cell Biol.* 6:434–441.

Salmon, E.D., E. Yeh, S. Shaw, B. Skibbens, and K. Bloom. 1998. High-resolution video and digital-enhanced differential interference contrast light microscopy of cell division in budding yeast. *Methods Enzymol.* 298:317–331.

Sambrook, J., E.F. Fritsch, and T. Maniatis. 1989. Molecular Cloning: A Laboratory Manual. Cold Spring Harbor Laboratory Press, Cold Spring Harbor, New York.

Sanders, S.L., and I. Herskowitz. 1996. The Bud4 protein of yeast, required for axial budding, is localized to the mother/bud neck in a cell cycle-dependent manner. *J. Cell Biol.* 134:413–427.

Sanders, S.L., M. Gentzsch, W. Tanner, and I. Herskowitz. 1999. *O*-glycosylation of Axl2p/Bud10p by Pmt4p is required for its stability, localization, and function in daughter cells. *J. Cell Biol.* 145:1177–1188.

Sikorski, R.S., and P. Hieter. 1989. A system of shuttle vectors and yeast host strains designed for efficient manipulation of DNA in *Saccharomyces cerevisiae*. *Genetics*. 122:19–27.

Sil, A., and I. Herskowitz. 1996. Identification of an asymmetrically localized determinant, Ash1p, required for lineage-specific transcription of the yeast *HO* gene. *Cell*. 84:711–722.

Spellman, P.T., G. Sherlock, M.Q. Zhang, V.R. Iyer, K. Anders, M.B. Eisen, P.O. Brown, D. Botstein, and B. Futcher. 1998. Comprehensive identification of cell cycle-regulated genes of the yeast *Saccharomyces cerevisiae* by microarray hybridization. *Mol. Biol. Cell.* 9:3273–3297.

Taheri, N., T. Köhler, G.H. Braus, and H.-U. Mösch. 2000. Asymmetrically localized Bud8p and Bud9p proteins control yeast cell polarity and development. *EMBO J.* 19:6686–6696.

Wach, A., A. Brachat, C. Alberti-Segui, C. Rebischung, and P. Philippsen. 1997. Heterologous *HIS3* marker and GFP reporter modules for PCR-targeting in *Saccharomyces cerevisiae*. *Yeast*. 13:1065–1075.

Zahner, J.E., H.A. Harkins, and J.R. Pringle. 1996. Genetic analysis of the bipolar pattern of bud site selection in the yeast *Saccharomyces cerevisiae*. *Mol. Cell. Biol.* 16:1857–1870.

JCB
Online Supplemental Material

Shenkman et al. http://www.jcb.org/cgi/doi/10.1083/jcb.200107041

Plasmid constructions

Previously used *BUD8* plasmids contained 290–540 bp of upstream sequence (Harkins, H.A., N. Pagé, L.R. Schenkman, C. De Virgilio, S. Shaw, H. Bussey, and J.R. Pringle. 2001. *Mol. Biol. Cell.* 12:2497–2518). To generate plasmids containing additional upstream sequence (a total of 1,410 bp, including the last 599 bp of upstream ORF *YLR352W* plus the 811 bp between this ORF and the *BUD8* start codon), this region was amplified by PCR using primers LS26 and LS27 (Table III) and genomic DNA from yeast strain YEF473 as template. The PCR product was digested with *Hin*dIII (one site included in primer LS26, the other included in the natural sequence upstream of *BUD8* and contained both in the PCR product and in the relevant plasmids) and subcloned into the *Hin*dIII site of plasmid YCpBUD8 (Harkins, H.A., N. Pagé, L.R. Schenkman, C. De Virgilio, S. Shaw, H. Bussey, and J.R. Pringle. 2001. *Mol. Biol. Cell.* 12:2497–2518), generating plasmid YCpBUD8F. The complete region upstream of *BUD8* in YCpBUD8F was sequenced to confirm its proper orientation and the absence of mutations introduced by the PCR. The *Hin*dIII fragment from YCpBUD8F was then subcloned into the *Hin*dIII sites of plasmids YCpHA-BUD8 and YEpGFP*-BUD8 (both described by (Harkins, H.A., N. Pagé, L.R. Schenkman, C. De Virgilio, S. Shaw, H. Bussey, and J.R. Pringle. 2001. *Mol. Biol. Cell.* 12:2497–2518), generating plasmids YCpHA-BUD8F and YEpGFP*-BUD8F, respectively; proper orientation of the *Hin*dIII fragments was confirmed by restriction-digest analysis. YEpGFP*-BUD8F, like YEpGFP-BUD8 (Harkins, H.A., N. Pagé, L.R. Schenkman, C. De Virgilio, S. Shaw, H. Bussey, and J.R. Pringle. 2001. *Mol. Biol. Cell.* 12:2497–2518), rescued the budding-pattern defect of a *bud8Δ/bud8Δ* strain.

To generate a plasmid expressing *GFP-BUD9*, a *Not*I fragment from YEpGFP*-BUD8 containing the *GFP* allele with the S65T, F64L, and V163A substitutions was used to replace the *Not*I fragment containing hemagglutinin (HA) sequences in YEpHA-BUD9 (Harkins, H.A., N. Pagé, L.R. Schenkman, C. De Virgilio, S. Shaw, H. Bussey, and J.R. Pringle. 2001. *Mol. Biol. Cell.* 12:2497–2518). The resulting plasmid, YEpGFP*-BUD9, contains *GFP* sequences inserted at an introduced *Not*I site directly downstream of the start codon in *BUD9*. YEpGFP*-BUD9, like YEpGFP-BUD9 (Harkins, H.A., N. Pagé, L.R. Schenkman, C. De Virgilio, S. Shaw, H. Bussey, and J.R. Pringle. 2001. *Mol. Biol. Cell.* 12:2497–2518), rescued the budding-pattern defect of a *bud9Δ/bud9Δ* strain.

Plasmids containing the *BUD8* or *BUD9* ORF expressed from the promoter of the other gene were constructed as follows. Plasmids YCpHA-BUD8F and YEpGFP*-BUD8F (see above) were digested with *Not*I and *Sac*I and ligated to the *BUD9*-containing *Not*I-*Sac*I fragment from YCpHA-BUD9 (Harkins, H.A., N. Pagé, L.R. Schenkman, C. De Virgilio, S. Shaw, H. Bussey, and J.R. Pringle. 2001. *Mol. Biol. Cell.* 12:2497–2518), generating plasmids $YCpP_{BUD8}$BUD9 and $YEpP_{BUD8}$BUD9, respectively. Similarly, plasmids YCpHA-BUD9 and YEpHA-BUD9 (Harkins, H.A., N. Pagé, L.R. Schenkman, C. De Virgilio, S. Shaw, H. Bussey, and J.R. Pringle. 2001. *Mol. Biol. Cell.* 12:2497–2518) were digested with *Not*I and *Sac*I and ligated to the *BUD8*-containing *Not*I-*Sac*I fragment from YEpGFP*-BUD8F, generating plasmids $YCpP_{BUD9}$BUD8 and $YEpP_{BUD9}$BUD8, respectively. In each of the starting plasmids used in these constructions, a *Not*I fragment containing the *HA* or *GFP* sequences was present at a *Not*I site that had been created by insertion of 9 bp immediately downstream of the *BUD8* or *BUD9* start codon (Harkins, H.A., N. Pagé, L.R. Schenkman, C. De Virgilio, S. Shaw, H. Bussey, and J.R. Pringle. 2001. *Mol. Biol. Cell.* 12:2497–2518). In plasmids YCpHA-BUD8F and YEpGFP*-BUD8F, the *Sac*I site was in the polylinker downstream of the *BUD8* sequences; in plasmids YCpHA-BUD9 and YEpHA-BUD9, the *Sac*I site was in the *BUD9*-region sequences, 143 bp downstream of the *BUD9* stop codon. Thus, plasmids $YCpP_{BUD8}$BUD9 and $YEpP_{BUD8}$BUD9 were expected to contain 1,410 bp of *BUD8* upstream sequence, a start codon plus 9 bp including the *Not*I site, the entire *BUD9* ORF (exclusive of the start codon), and 143 bp of *BUD9* downstream sequence. Similarly, plasmids $YCpP_{BUD9}$BUD8 and $YEpP_{BUD9}$BUD8 were expected to contain 813 bp of *BUD9* upstream sequence, a start codon plus 9 bp including the *Not*I site, the entire *BUD8* ORF (exclusive of the start codon), and 404 bp of *BUD8* downstream sequence. Restriction-digest analysis of the newly generated plasmids confirmed that the *HA* and *GFP* sequences were indeed absent. Finally, the *GFP*-containing *Not*I fragment from pKS-GFP* (Harkins, H.A., N. Pagé, L.R. Schenkman, C. De Virgilio, S. Shaw, H. Bussey, and J.R. Pringle. 2001. *Mol. Biol. Cell.* 12:2497–2518) was subcloned into $YEpP_{BUD8}$BUD9 and $YEpP_{BUD9}$BUD8, generating plasmids $YEpP_{BUD8}$GFP*-BUD9 and $YEpP_{BUD9}$GFP*-BUD8, respectively, which should express *GFP-BUD8* or *GFP-BUD9* from the promoter of the other gene.

To construct an integrative plasmid containing the *HA-BUD8* coding region directly downstream of the *BUD9* upstream sequences, the *Sph*I-*Sac*I fragment from $YEpP_{BUD9}$BUD8 (*Sph*I site from the vector polylinker upstream of the *BUD9* upstream sequences; *Sac*I site as described above) was subcloned into the *URA3*-containing integrating plasmid YIplac211, generating plasmid $YIpP_{BUD9}$BUD8. A *Not*I fragment containing the triple *HA* epitope sequence was then subcloned from YCpHA-BUD9 into $YIpP_{BUD9}$BUD8, generating plasmid $YIpP_{BUD9}$HA-BUD8.

Table III. **Oligonucleotide primers used in this study.**

Primer	Sequence[a]
LS26	5′-GGGGGCCCCCATAAGCTTACAGTCATGTGGAAGATAGCC-3′[b]
LS27	5′-GTATACCGGTAATCGCCTAG-3′
LS72	5′-CGACGGCCAGTGAATTGTAATACGACTCACTATAGGGCGACGGCCAGTGAATTCGAGCTC-3′
LS73	5′-CATAGGAATAGGATTTGGTGTGGGAATAACAAGAGAGTAAGAAACTGTATCATTCATCAAATAG-3′
LS84	5′-TCAAGAAATTGATCGAGATCAGCAATTAAGTTTTCAAATGGAGGCGAGAATGCCAATTCA-3′
LS85	5′-TAGGAAAGAAGACAGGCACGATGCTGAAAACATAGACCTGGAAACAATGCCCATTCAAAG-3′
LS86	5′-GTTTTTATTTTTTATCCTATTTGATGAATGATACAGTTTCTTACTCTCTTGTTATTCCCA-3′
LS89	5′-AATGAATTCACCATCTTCGCAGAGATTAAGTTGCGCACTGACCATCTCTACTTCGGTGCT-3′
LS93	5′-GGACTCTTCTGAAACGACAGC-3′
LS94	5′-CTTCATCCTCGGTCTCGCC-3′
LS95	5′-CATCCACATCTGGATCGGC-3′
LS96	5′-CACCATACCGCATAGAAGG-3′
LS100	5′-CTAGGCGATTACCGGTATAC-3′
LS101	5′-ATCCAGCCTTCTCTGGGATTTTTAGTTTGTGCGGTATAAACGCTTTATCGGGAAAAGTAC-3′
LS102	5′-AAAATTTATACCGCACAAACTAAAAATCCCAGAGAAGGCTTGGAACAGAATACCAGCGAA-3′
LS112	5′-CCACTGTAGACGAGAGGCC-3′
LS113	5′-CTATATTACTTGGGTATTGCC-3′
LS114	5′-GAGGAATGTACAAAGGTTGGC-3′
LS115	5′-CTTCTGCATCTAGGTCTTCC-3′
LS129	5′-TTCCGCTGAAACTAACCTAAATGGACACAGCAGCAGCGGTACAATATCAACTTCAGTTCT-3′
LS130	5′-TTTTGAGGCTAGTGGATTTATTCGCTGGTATTCTGTTCCAAGCCTTCTCTGGGATTTTTA-3′
LS158	5′-GTGCGGCCGCATCTTTTACCC-3′
LS159	5′-CGTGCGGCCGCACTGAGCAGC-3′
LS174	5′-CATCGCTTAGAAATATTTGGCTAGGAAACATTAGGACTAACGGATCCCCGGGTTAATTAA-3′
LS175	5′-TATCTGATATCTTGATTCATTTATAATAAAATTAAGTGAGAATTCGAGCTCGTTTAAAC-3′
LS183	5′-TTTTGACTGAAGCTCCAATGAACCCTAAAT-3′
LS184	5′-ACGGACATCGACATCACACTTCATGATGGC-3′
LS269	5′-CAGTCATGTGGAAGATAGCCAAAATCACGTGAATGCCATCCCTGTTCTTGACCGTCTAC-3′
LS270	5′-AGTCCAAATTATCTTCGTCTGATTGTATGCGGCCGCCCATCTATAAGATCAATGAAGAG-3′
LS271	5′-GTCATGTGGAAGATAGCCAAAATCACGTGAATGCCATCCGTGATTTTCACCGAGCGAC-3′
LS272	5′-GTCCAAATTATCTTCGTCTGATTGTATGCGGCCGCCCATTGTCTGTCGTTAAATTTAAT-3′
LS273	5′-GTACCCGGGGATCCTCTAGAGTCGACCTGCATGCCAATGGCCTGTTCTTGACCGTCTAC-3′
LS274	5′-TTATCGAAACATCTCTGGTTATTTTCGTGCGGCCGCACATCTATAAGATCAATGAAGAG-3′
LS275	5′-GTACCCGGGGATCCTCTAGAGTCGACCTGCATGCCAATGGCGTGATTTTCACCGAGCGA-3′
LS276	5′-TATCGAAACATCTCTGGTTATTTTCGTGCGGCCGCACATTGTCTGTCGTTAAATTTAAT-3′

[a]The sequences used to direct homologous recombination are underlined.
[b]The *Hin*dIII site is indicated in bold face.

Other plasmid constructions used the following general strategy. First, a DNA fragment was generated by PCR that contained the sequences to be inserted bounded by ends (~40 bp each) corresponding to the desired recombination sites in a target plasmid. This plasmid was digested at a unique restriction site located within the domain to be replaced and cotransformed along with the PCR fragment into yeast strain YEF473, selecting for the desired recombinant plasmid (Ma, H., S. Kunes, P.J. Schatz, and D. Botstein. 1987. *Gene.* 58:201–216; Oldenburg, K.R., K.T. Vo, S. Michaelis, and C. Paddon. 1997. *Nucleic Acids Res.* 25: 451–452). After rescue of plasmids into *Escherichia coli*, the appropriate regions were sequenced to confirm the desired replacement of sequences and the absence of errors introduced by the PCR.

To construct plasmid YCpP_{BUD8}BUD9*, primers LS73 and LS72 were used with plasmid YCpBUD8F as template to generate a fragment that contained 404 bp of *BUD8* downstream sequence beginning immediately after the stop codon. This fragment was cotransformed along with YCpP_{BUD8}BUD9 that had been digested at its unique *Sac*I site (at the junction between the *BUD9* downstream sequence and the vector sequences). Primer LS73 contains sequences at its 5′ end corresponding to the 3′ end of the *BUD9* ORF, and primer LS72 contains sequences at its 5′ end that correspond to vector sequences just beyond the *Sac*I site in YCpP_{BUD8}BUD9. Thus, YCpP_{BUD8}BUD9* is identical to YCpP_{BUD8}BUD9 except that it contains *BUD8* rather than *BUD9* downstream sequence.

To construct plasmids containing *BUD8* or *BUD9* expressed from the *CLB2* or *CLN2* promoter, YCpHA-BUD8F and YCpHA-BUD9 (see above) were first digested with *Not*I and religated, thus removing the *HA* sequences and creating plasmids YCpBUD8-NotI and YCpBUD9-NotI. Genomic DNA from strain YEF473 was then used as template to generate fragments containing the 996 bp immediately upstream of the *CLB2* ORF or the 996 bp immediately upstream of the *CLN2* ORF. The primers contained sequences at their 5′ ends corresponding either to the complement of the 5′ end of the *BUD8* or *BUD9* ORF or to the vector sequences upstream of the *BUD8* or *BUD9* upstream sequences in plasmid YCpBUD8-NotI or YCpBUD9-NotI. The PCR products were then cotransformed along with either YCpBUD8-NotI or YCpBUD9-NotI that

had been digested within the *BUD8* or *BUD9* upstream sequences by *Bam*HI or *Sna*BI, respectively. Primer pairs LS269 and LS270, LS271 and LS272, LS273 and LS274, and LS275 and LS276 were used to construct plasmids $YCpP_{CLB2}$BUD8, $YCpP_{CLN2}$BUD8, $YCpP_{CLB2}$BUD9, and $YCpP_{CLN2}$BUD9, respectively.

To construct plasmids YCpBUD8/9-1, YCpBUD8/9-3, and YCpBUD8/9-5, primer pairs LS85 and LS86, LS102 and LS86, and LS89 and LS86, respectively, were used with plasmid YCpBUD9 as template to generate fragments of the *BUD9* coding region that extended from nucleotides 1,288, 847, and 472 (all relative to the A of the start codon), respectively, through the stop codon. Primers LS85, LS102, and LS89 contain sequences at their 5′ ends that correspond to the *BUD8* coding region at nucleotides 1,407–1,446, 819–858, and 432-471 (all relative to the start codon), respectively, whereas primer LS86 contains sequences at its 5′ end that correspond to the complement of the beginning of the *BUD8* downstream sequences. Each PCR product was cotransformed along with YCpBUD8-NotI that had been digested at its unique *Pst*I site (nucleotides 1,599–1,604 of the *BUD8* ORF). Thus, each resulting plasmid contains 1,410 bp of *BUD8* upstream sequence; a start codon plus 9 bp including the *Not*I site; the first 1,443, 855, or 468 bp of *BUD8* coding sequence (excluding the start codon) fused to the last 357, 798, or 1,173 bp, respectively, of the *BUD9* ORF; and 404 bp of *BUD8* downstream sequence.

To construct plasmid YCpBUD8/9-2, primers LS84 and LS72 were used with plasmid YCpBUD8F as template to generate a fragment that contained *BUD8* sequence extending from nucleotide 1,447 (relative to the start codon) to 404 bp downstream of the stop codon. This fragment was cotransformed along with $YCpP_{BUD8}$BUD9 that had been digested at its unique *Nhe*I site (nucleotides 1,600–1,605 of the *BUD9* ORF). Primer LS84 contains sequences at its 5′ end that correspond to nucleotides 1,248–1,287 of the *BUD9* ORF; primer LS72 is described above. Thus, plasmid YCpBUD8/9-2 contains the *BUD8* upstream and downstream sequences surrounding an ORF that consists of a start codon plus 9 bp including the *Not*I site, the first 1,284 bp of the *BUD9* ORF (excluding the start codon), and the last 363 bp of the *BUD8* ORF.

To construct plasmid YCpBUD8/9-4, primers LS100 and LS101 were used with plasmid $YCpP_{BUD8}$BUD9 as template to generate a fragment that contained the 189 bp of *BUD8* upstream sequences immediately upstream of the start codon, the start codon plus 9 bp including the *Not*I site, and the following 807 bp of *BUD9* coding sequence. This fragment was cotransformed along with YCpBUD8/9-1 that had been digested at the unique *Not*I site. Primer LS101 contains sequences at its 5′ end that correspond to the complement of nucleotides 823–862 of the *BUD8* ORF. Thus, plasmid YCpBUD8/9-4 contains the *BUD8* upstream and downstream sequences surrounding an ORF that consists of a start codon plus 9 bp including the *Not*I site, the first 807 bp of the *BUD9* ORF (excluding the start codon), base pairs 823–1,446 of the *BUD8* ORF, and the final 357 bp of the *BUD9* ORF.

To construct plasmid YCpBUD8/9-6, primers LS129 and LS130 were used with plasmid YCpBUD8F as template to generate a fragment that contained base pairs 472–858 (relative to the start codon) of the *BUD8* ORF. This fragment was cotransformed along with $YCpP_{BUD8}$BUD9 that had been digested at its unique *Nde*I site (base pairs 541–546 of the *BUD9* ORF). Primers LS129 and LS130 contain sequences at their 5′ ends corresponding to nucleotides 432–471 and the complement of nucleotides 847–886, respectively, of the *BUD9* ORF. Thus, plasmid YCpBUD8/9-6 contains the *BUD8* upstream sequences and *BUD9* downstream sequences surrounding an ORF that consists of a start codon plus 9 bp including the *Not*I site, the first 468 bp of the *BUD9* ORF (excluding the start codon), base pairs 472–858 of the *BUD8* ORF, and the final 798 bp of the *BUD9* ORF.